Cathodoluminescence of meteoritic and synthetic forsterite at 296 and 77 K using TEM

E.J. BENSTOCK,[1] PETER R. BUSECK,[1,2] AND IAN M. STEELE[3]

[1]Department of Geology, Arizona State University, Tempe, Arizona 85287-1404, U.S.A.
[2]Department of Chemistry and Biochemistry, Arizona State University, Tempe, Arizona 85287-1404, U.S.A.
[3]Department of Geophysical Sciences, University of Chicago, Chicago, Illinois 60637, U.S.A.

ABSTRACT

Cathodoluminescence (CL) emission spectra of forsterite from the Allende (CV3) and Murchison (C2) meteorites and from Cr-doped and pure synthetic forsterite samples have been obtained at room (296 K) and liquid nitrogen (77 K) temperatures using a transmission electron microscope. At room temperature, three broad CL emissions centered near 420, 640, and 800 nm occur in the meteoritic forsterite, and one peak at 800 nm occurs in one Cr^{3+}-doped forsterite sample. Only the 420 nm peak is present in pure synthetic forsterite. Relative to room temperature, at liquid-nitrogen temperature there is a general increase in overall CL intensity, whereas a broad peak located between 700 and 800 nm changes to a series of sharp emissions centered near 700 nm and a narrower but still broad peak centered near 800 nm.

The portion of the broad peak near 700 nm at room temperature and equivalent sharp peaks at low temperature are assigned to Cr^{3+} in octahedral coordination, whereas the broad peak near 800 nm is attributed to Cr associated with structural defects. The peak at 640 nm is consistent with a similar peak in Mn^{2+}-doped forsterite. The peak at 420 nm results from an unknown structural effect that can be eliminated in synthetic forsterite by mechanical deformation. The variation of relative intensities at room temperature for the two broad peaks at 700 and 800 nm in meteoritic forsterite can be correlated with meteorite type and may reflect different processes in forsterite formation or subsequent processing.

INTRODUCTION

Nearly pure forsterite occurs both as single grains in the matrices of primitive meteorites and within chondrules and inclusions (Steele 1986a), but its origin remains controversial (McSween 1977; Olsen and Grossman 1978; Jones 1992). Such forsterite is particularly easy to recognize because it shows cathodoluminescence (CL), usually seen using an electron microprobe or luminescence microscope. Steele et al. (1985) and Steele (1986a, 1989, 1992) described CL in forsterite from primitive meteorites and micrometeorites and correlated the CL color with chemical composition. The Mg-rich core with less than about 2 wt% FeO is enriched in minor amounts of Al, Ca, V, Ti, and Sc relative to the rim, which contains more Cr and Mn and up to ~30 wt% FeO. These forsterite cores show CL but the rims do not because high Fe^{2+} concentrations quench CL. Patterns of CL within meteoritic forsterite have also been described that correspond to oscillatory zoning, with the implication that these grains crystallized from a melt (Steele 1995). Synthetic Cr-doped forsterite is an important material for tunable lasers (Petričević et al. 1989), and CL may prove to be a useful technique for characterization of some of its chemical and physical properties.

CL emissions result from several sources, including electronic transitions among d and f energy levels and transitions among energy levels caused by various types of structural defects. It can be difficult to ascribe particular CL emissions to any one effect, but a correlation among color, intensity, and composition is strong evidence for a cause-effect relationship. For example, synthetic samples doped with a single activating ion may provide a reference for a wavelength that is characteristic of that ion in a particular site in that material. The intensity calibration is more difficult because it is not a simple function of concentration but rather is affected by other elements (Marshall 1988). Because transition metal ions with unfilled d shells (e.g., Cr and Mn) occur in forsterite that shows CL, they are logical candidates for correlation with CL properties. Complications may occur because some elements in the first transition series can have multiple oxidation states (e.g., Cr, Ti, V), and their ions may substitute in more that one crystallographic site, each with different energy levels that result from different coordination (Burns 1993).

CL spectra are typically obtained using the electron microprobe, which may allow correlation with composition. However, uncertainties arise because some elements that cause CL may be below the detection level of the electron microprobe. The TEM also generates CL, with the added advantages that significantly higher spatial resolution is possible, samples can be cooled, and micro-

structural information obtained using standard TEM techniques for thinned samples. Cooling reduces both phonon broadening of the CL peaks and electron-beam damage to the sample. Although these added advantages of the TEM were not exploited in this study, they potentially allow the examination of CL from either small samples or localized areas of intergrowths. For the present study, spatial resolution was not considered critical, but rather we were most interested in both reproducing observations made by other instruments and documenting the effects of sample cooling, which could easily be done in our instrument and could be applied to very small samples.

The goals of the present research are to determine the contribution of Cr^{3+} to the CL of forsterite, to examine the wavelength of CL in forsterite from different types of meteorites, and to provide additional observations for the blue component of CL, which is present in many materials, including forsterite. Because this is the first TEM study of silicate minerals using CL, we compared our results with CL data obtained using an electron microprobe.

EXPERIMENTAL METHODS

Thin sections of the Allende and Murchison meteorites were examined with a JEOL JXA 8600 electron microprobe to locate luminescent olivine samples. Although the compositions of these grains were not obtained, the range of forsterite compositions that show CL is well established (Steele 1989): specifically, Fe, <2 wt%; Cr_2O_3, 1000–2000 ppmw; TiO_2, 100–500 ppmw; Al_2O_3, 0.1–0.6 wt%; CaO, 0.4–0.7 wt%; Sc_2O_3, <130 ppmw; and V_2O_3, <500 ppmw. Luminescent grains in both meteorites may occur either as single isolated grains or as relict grains within chondrules, but single grains are far more common and represent our analyzed material. Selected grains were ion milled using VCR Group 306B or Gatan 600 ion mills. Both Cr^{3+}-doped and undoped synthetic forsterite samples were also prepared by ion milling and by crushing of forsterite in a suspension with ethanol.

For the CL measurements we used a Philips 400T TEM, equipped with a CL detection system designed and described by Yamamoto et al. (1983). Operating conditions for the TEM were 120 kV accelerating voltage, ~1 µA emission current, 70 µm condenser aperture, and 14 µm beam diameter. For CL, the acquisition time was 200 ms using a 0.5 mm entrance slit, giving a spectral resolution of ~2 nm. Samples were cooled by a liquid nitrogen holder. We were interested in the qualitative spectral changes and the effect of low temperatures; therefore, the spectra did not need to be corrected for detector response or optimized for spectral resolution.

RESULTS

The TEM CL spectrum of Allende forsterite at room temperature contains three broad emissions located near 410, 630, and 790 nm (Fig. 1). The presence and wavelengths of these peaks are similar to those previously shown for meteoritic forsterite from several meteorites
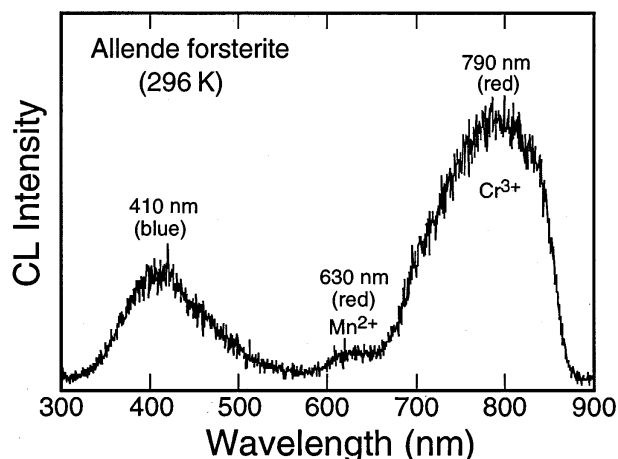

FIGURE 1. Cathodoluminescence spectrum of Allende forsterite at 296 K. Three broad emissions centered near 410, 630, and 790 nm are apparent. The sharp drop in intensity near 880 nm results from low transmission and sensitivity of the detector for infrared wavelengths. Although not apparent in this spectrum, there is a similar loss of sensitivity in the ultraviolet region. The assignments of peaks to Cr and Mn are based on the data of Steele (1988a).

(Steele 1986b). For very broad peaks, an exact correspondence between the present spectra and those of Steele (1986b) should not be expected. Differences result because the detectors have different sensitivity functions, and these can change the apparent positions of maxima for broad peaks; in particular, the detector described by Yamamoto et al. (1983) was reported to be sensitive in the UV region, whereas the detector used by Steele (1986a) was not. This difference would tend to show peak maxima at lower wavelength for the UV-sensitive detector. At liquid nitrogen temperature (~77 K), the Allende forsterite spectrum shows a series of sharp peaks between 680 and 720 nm, an intense, broad peak centered near 800 nm (Fig. 2) and a broad peak in the blue spectral region. Synthetic Cr^{3+}-doped forsterite (Fig. 3) and Murchison forsterite (Fig. 4) also display sharp peaks in the 680–720 nm region at 77 K. Figure 2 and especially Figures 3 and 4 suggest that at 296 K the broad peak between 650 and 850 nm is composed of two broad peaks on the basis of occurrence of an inflection point in the profile. The one at shorter wavelength is near the same position where a series of sharp peaks appear at low temperature, whereas the broad peak at higher wavelength remains broad at the low temperature. Spectra of undoped synthetic forsterite have neither these sharp peaks nor the broad 800 nm peak at either high or low temperatures.

The details of the 680–720 nm region for Allende, Murchison, and Cr^{3+}-doped forsterite samples are compared in Figure 5 with an expanded wavelength scale. There is a close correspondence among these spectra, both in the wavelengths and relative intensities of peaks.

The CL emission in the blue region near 420 nm is conspicuous in the spectra of Allende forsterite (Figs. 1
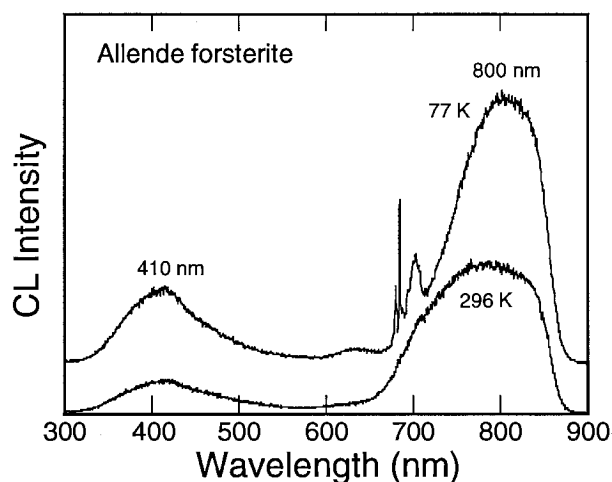
FIGURE 2. Comparison of Allende forsterite CL spectra at 77 and 296 K, obtained from the same region of crystal and plotted on the same intensity scale. It is clear that the overall intensity is approximately doubled, and the broad peak centered near 800 nm changes to a series of sharp emissions in addition to a broad emission with consequent changes in peak shape at low temperature. The 296 K spectrum is not that shown in Figure 1 and shows no apparent peak near 630 nm.

and 2) but weak to nonapparent in the synthetic (Fig. 3) and Murchison (Fig. 4) forsterite samples. The synthetic undoped forsterite prepared by ion milling shows a strong emission in the blue region (Fig. 6). For the same sample was prepared by crushing, the blue emission is absent and only a small but continuous increase in emission toward
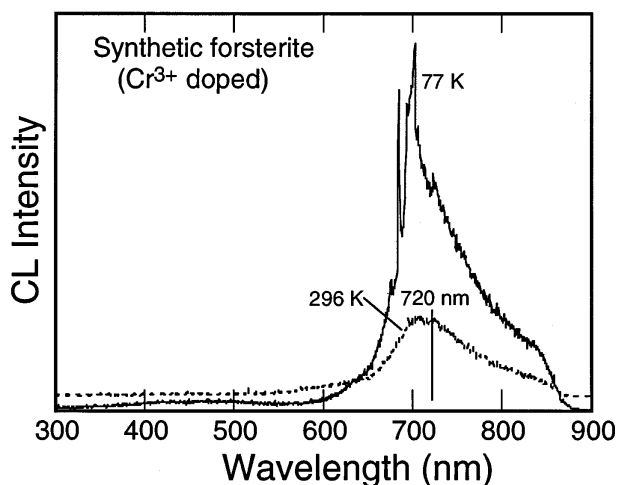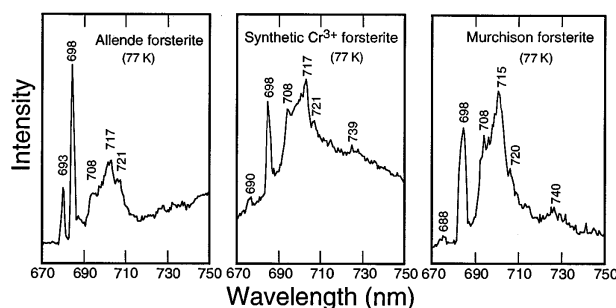

FIGURE 3. Comparison of CL spectra from Cr^{3+}-doped synthetic forsterite at 77 and 296 K. The broad emission between 680 and 800 nm at 296 K indicates two overlapping peaks. At 77 K, a series of sharp peaks appears between 680 and 720 nm superimposed on a broad emission, the exact position of which is not certain. A weak peak near 400–500 nm is present, and an overall increase in intensity occurs at low temperature. Spectra are displaced vertically to reduce overlap.
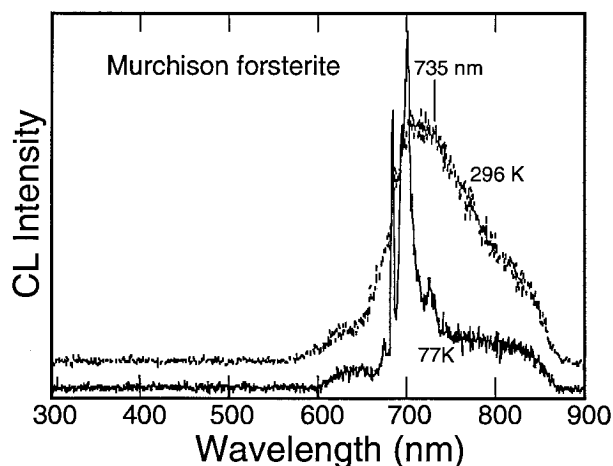
FIGURE 4. Comparison of CL spectra from Murchison forsterite at 77 and 296 K. At 296 K, a broad emission consists of an intense peak near 720 nm and weaker peaks near 640 and 800 nm. At low temperatures, a series of sharp emissions appears near 700 nm. The broad peaks at 640 and 800 nm remain but with reduced intensity relative to those at high temperature. Spectra are displaced vertically to reduce overlap.

the infrared is present until the detector sensitivity decreases near 870 nm. These observations strongly suggest that this blue emission is not due to an activator ion but is rather associated with another property that is sensitive to deformation. Although this is not our main interest, the possibility of using the TEM to characterize the deformed material is an obvious direction for future studies.

Recent attempts to duplicate the results reported here using an electron microprobe with a cold stage have had mixed success (Vasconcellos and Steele 1996). The microprobe results indicate an effect of accelerating voltage on the resulting CL spectra, where the red portion of the spectrum is enhanced relative to the blue for an increase from 15 to 30 kV. Because Vasconcellos and Steele (1996) were limited to 30 kV, it was not possible to ap-

FIGURE 5. Comparison of CL line spectra near 700 nm for Allende, Cr^{3+}-doped and Murchison forsterite, obtained at low temperature. The three spectra closely correspond in peak positions and relative intensities; these peaks also occur at approximately the same positions as a series of narrow line peaks observed for forsterite at low temperature by Moncorgé et al. (1991).

proach the conditions used here (120 kV). In addition, the sharp spectra reported here were not obtained by them, although the microprobe temperatures approached those of liquid nitrogen. There was, however, a definite narrowing of peaks and a hint of sharp emissions, but these do not approach the intensities reported here. We tentatively conclude that the accelerating voltage has an important effect on CL spectra.

DISCUSSION

The room-temperature TEM CL spectra of Allende forsterite are similar to those obtained by Steele (1986a) using an electron microprobe. Both sets of spectra show a broad red CL emission near 800 nm and a second broad emission in the blue region centered near 420 nm in the TEM measurements and near 450 nm in the microprobe data. Because different CL detectors have different transmission efficiencies as a function of wavelength, and neither our spectra nor those of Steele were corrected for instrumental response, we interpreted the 420 nm TEM CL peak to be equivalent to the 450 nm peak in the microprobe spectra. The small 640 nm peak correlates with the Mn peak reported by Steele (1988a) for synthetic, Mn-doped forsterite.

The sharp peaks that appear in the red end of the spectrum at low temperature are at almost identical wavelengths in the Allende, Murchison, and Cr^{3+}-doped synthetic forsterite samples (Fig. 5). This similarity suggests that the cause of these peaks is the same in all three samples. These peaks are not present in the pure synthetic forsterite (Fig. 6). Fluorescence spectra reported by Moncorgé et al. (1991) for synthetic Cr^{3+}-doped forsterite likewise show a series of sharp emission peaks centered near 700 nm in a cooled sample, which at room temperature formed only a broad emission centered near this same wavelength. The number and wavelengths of these peaks also resemble those attributed to Cr^{3+} in octahedral coordination in spinel, ruby, garnets, and emerald (Wood et al. 1968; Sviridov et al. 1973). Slight shifts in the wavelengths and spacings of these peaks from different minerals could result from different crystal fields and site coordinations in each structure. We thus conclude, like Moncorgé et al. (1991), that the broad peak near 700 nm at room temperature and the series of sharp peaks at low temperature result from Cr^{3+} in octahedral coordination, either the M1 or M2 cation sites, or both, in the forsterite structure.

The 800 nm emission observed both at room temperature and at low temperature in the spectra of the Allende, Murchison, and synthetic Cr^{3+}-doped forsterite samples closely matches the broad emission described by Moncorgé et al. (1991). This peak does not occur in the pure synthetic forsterite (Fig. 6). The similar appearance at room and low temperatures, in contrast to the 700 nm emission, suggests that it is related to Cr, but the origin of the CL differs from that causing the 700 nm peak; Moncorgé et al. (1991) assigned this emission to Cr^{3+} but associated with charge vacancies.
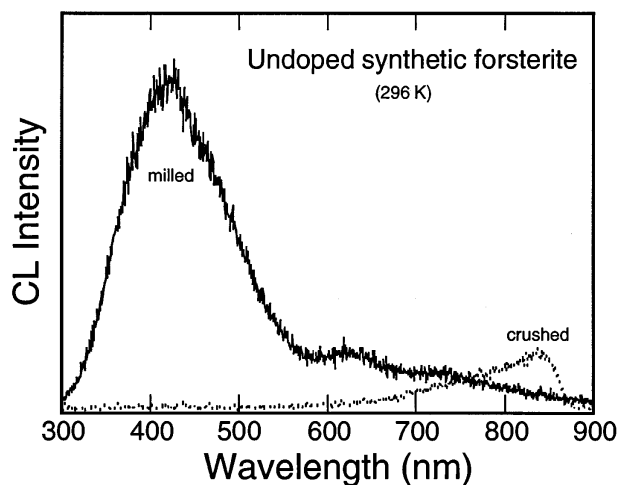

FIGURE 6. Effect of sample preparation of pure forsterite on intensity of blue peak near 420 nm. The peak in the ion-milled sample is not present in a sample prepared by simple crushing, illustrating an effect that is possibly produced by simple mechanical deformation.

At room temperature that part of the visible CL spectrum attributed to Cr^{3+} in meteoritic forsterite consists of two broad unresolved peaks: one centered near 700 nm, the other near 800 nm. Evidence of these two peaks can be seen in Figures 3 and 4, where in the room-temperature spectra a weak shoulder on the peak near 700 nm is indicated by an inflection in the profile near 770 nm. When these two broad peaks are similar in intensity only a single, very broad peak is present as in Figure 2. For the Allende and Murchison forsterite samples, the intensities of the two broad peaks that result from Cr are not the same. For example, in Figure 2 (Allende forsterite) the peak near 800 nm is more intense than that near 700 nm, whereas in Figures 3 and 4 the peak near 700 nm is more intense than that near 800 nm. In general, the combination of these two Cr-related peaks gives a single broad peak, the position of which ranges from near 700 to near 800 nm depending on the individual intensities of the two contributing broad peaks.

Steele (1988b) observed that, on the basis of room-temperature spectra, there is a systematic shift in the position of the peak maximum of the broad emission in the 700–800 nm region of natural forsterite from a variety of extraterrestrial samples. In his data, forsterite of Allende and other C3 meteorites as well as unequilibrated ordinary chondrites show the position of this peak near 780 nm. In contrast, forsterite of C2 meteorites has a peak position between 740 and 760 nm. This shift can be interpreted as a change in the relative intensities of the two contributing Cr^{3+} broad peaks to the resultant broad emission.

The above interpretation is consistent with data reported for synthetic Cr-doped forsterite grown under oxidizing conditions, but forsterite in meteorites was formed in highly reducing conditions where both Cr^{2+} and Cr^{3+}

would be stable and incorporated into the forsterite structure. In lunar olivines, which formed under reducing conditions similar to those thought to be present during meteorite formation, the occurrence of both Cr^{2+} and Cr^{3+} has been documented (Sutton et al. 1993). Likewise, olivine in chondrules has been shown to contain both Cr^{2+} and Cr^{3+} (Sutton et al. 1996). In contrast, under oxidizing conditions Cr^{4+} is thought to be present in tetrahedral coordination replacing Si^{4+} and is mainly responsible for the laser properties of forsterite (Petričević et al. 1989; Rager et al. 1991). Because the CL spectra of synthetic Cr^{3+}-doped forsterite and meteoritic forsterite appear similar, we conclude that neither Cr^{2+} nor Cr^{4+} has a significant effect on the CL spectra and that Cr^{3+} is the principal influence.

The changes in the relative intensities of the two CL peaks resulting from Cr^{3+} substitution suggest that structural information is reflected in the CL spectra. Forsterite in C2 meteorites and that in C3 meteorites can be distinguished by their minor element signatures (Steele and Smith 1986), and we propose that these chemical differences are also reflected in the CL spectra. The forsterite CL spectra from C2 meteorites and other related extraterrestrial forsterite samples with minor element contents similar to those of C2 meteorites (Steele 1988b) are dominated by an emission near 700 nm. On the basis of the above interpretation, the CL of these samples is mainly due to Cr^{3+} in octahedral coordination. In contrast, forsterite from C3 and unequilibrated ordinary chondrites shows CL dominated by the emission near 800 nm, which is attributed to Cr^{3+} interacting with nearby vacancies (Moncorgé et al. 1991). Although these CL characteristics allow classification of individual forsterite grains (Steele 1988b), they also suggest different structural environments for Cr^{3+}. Possible factors that may affect the structural environment of Cr include the following: (1) the mode of formation, either growth from a melt or condensation from a vapor; (2) subsequent thermal processing during chondrule formation; and (3) irradiation of isolated grains in a nebula. Although none of these can be demonstrated with certainty, the CL spectra provide additional clues to the origin of these olivine grains.

In Allende and also in Murchison forsterite, a broad but weak peak occurs near 640 nm. At low temperature this peak remains broad (Figs. 2 and 4). By comparison with synthetic Mn-doped forsterite (Steele 1988a), this peak is assigned to Mn almost certainly in octahedral coordination and probably concentrated in the M2 site (McCormick et al. 1987). In principle, the emission should differ between Mn sited on M1 and M2, and the position and shape of the emission peaks may reflect occupancy factors. A similar study was conducted for dolomite (El Ali et al. 1993), where deconvolution of a doublet allowed Mn occupancy to be determined between the two nonequivalent sites in this carbonate.

Although electron spin resonance was used to determine the actual Mn distribution in dolomite, ALCHEMI (atom location by channeling-enhanced microanalysis) has been used to determine site occupancy of minor elements in olivine (Taftø and Spence 1982; McCormick et al. 1987; Buseck and Self 1992). In principle, both ALCHEMI and CL data could be obtained with the TEM and correlated. However, because Mn is strongly partitioned into M2, the variation of CL peak position and shape may not be sensitive enough to record occupancy variations.

Allende, Cr^{3+}-doped, and pure forsterite show a broad CL emission near 420 nm whereas Murchison forsterite does not. It is also apparent that the peak in pure forsterite is dramatically affected by sample preparation for TEM analysis. Many Fe-poor and Fe-free silicates show blue luminescence, e.g., quartz, feldspars, melilite, Ca-rich garnet, enstatite, and forsterite; in addition, many nonsilicates show similar blue CL. Marfunin (1979) proposed that blue CL in anorthite may be caused by Al-O⁻-Al centers. Likewise, the blue CL in forsterite may be caused by Al-O⁻ centers, as Al^{3+} substitutes for Si^{4+} in Allende olivines (Steele 1986b). An SEM CL study of quartz was performed by Hanusiak and White (1975), who used molecular orbital calculations to support their conclusion that a 450 nm CL peak that is omnipresent in quartz is a result of molecular orbital energy levels of the SiO_4^{4-} tetrahedron. Geake et al. (1971), on the other hand, suggested that the blue CL in plagioclase and other silicates is caused by lattice defects. The fact that the ion-milled sample gave the characteristic 420 nm peak, whereas the crushed sample did not, suggests that the activating electronic structure that creates the blue CL is destroyed by mechanical deformation, such as crushing; it is also possible that an electronic configuration caused by mechanical deformation absorbs the CL emission and releases the energy nonradiatively.

It has been suggested (Marshall 1988) that this common blue peak is not caused by an activator ion, in part because many pure materials, including quartz, do not contain activator impurities. The absence of this blue peak in the Murchison CL spectrum (Fig. 4) may point to a particular process that these forsterite samples have experienced, analogous to the modification of the synthetic forsterite by crushing, but further work is required to explain the details.

REFERENCES CITED

Burns, R.G. (1993) Mineralogical applications of crystal field theory, 551 p. Cambridge University Press, New York.

Buseck, P.R., and Self, P. (1992) Electron energy loss spectroscopy (EELS) and electron channeling (ALCHEMI). In Mineralogical Society of America Reviews in Mineralogy, 27, 141–180.

El Ali, A., Barbin, V., Calas, G., Cervelle, B., Ramseyer, K., and Bouroulec, J. (1993) Mn^{2+}-activated luminescence in dolomite, calcite and magnesite: Quantitative determination of manganese and site distribution by EPR and CL spectroscopy. Chemical Geology, 104, 189–202.

Geake, J.E., Walker, G., Mills, A.A., and Garlick, G.F.J. (1971) Luminescence of Apollo lunar samples. Proceedings of the Second Lunar Science Conference, Geochimica et Cosmochimica Acta, Supplement 2, 2265–2275.

Hanusiak, W.M., and White, E.W. (1975) SEM cathodoluminescence for characterization of damaged and undamaged α-quartz in respirable dusts. Scanning Electron Microscopy, Part I, 125–132.

Jones, R.H. (1992) On the relationship between isolated and chondrule olivine grains in the carbonaceous chondrite ALHA 77307. Geochimica et Cosmochimica Acta, 56, 467–482.

Marfunin, A.S. (1979) Spectroscopy, Luminescence and radiation centers in minerals, 352 p. Springer-Verlag, New York.

Marshall, D.J. (1988) Cathodoluminescence of geologic materials, 146 p. Unwin Hyman, Boston.

McCormick, T.C., Smyth, J.R., and Lofgren, G.E. (1987) Site occupancies of minor elements in synthetic olivines as determined by channeling-enhanced X-ray emission. Physics and Chemistry of Minerals, 14, 368–372.

McSween, H.Y. (1977) On the nature and origin of isolated olivine grains in carbonaceous chondrites. Geochimica et Cosmochimica Acta, 41, 411–418.

Moncorgé, R., Cormier, G., Simkin, D.J., and Capobianco, J.A. (1991) Fluorescence analysis of chromium-doped forsterite (Mg_2SiO_4). Institute of Electrical and Electronics Engineers Journal of Quantum Electronics, 27, 114–120.

Olsen, E., and Grossman, L. (1978) On the origin of isolated olivine grains in type 2 carbonaceous chondrites. Earth and Planetary Science Letters, 41, 111–127.

Petričević V., Gayen, S.K., and Alfano, R.R. (1989) Continuous-wave laser operation of chromium-doped forsterite. Optics Letters, 14, 612–614.

Rager, H., Taran, M., and Khomenko, V. (1991) Polarized optical absorption spectra of synthetic chromium doped Mg_2SiO_4 (forsterite). Physics and Chemistry of Minerals, 18, 37–39.

Steele, I.M. (1986a) Compositions and textures of relic forsterite in carbonaceous and unequilibrated ordinary chondrites. Geochimica et Cosmochimica Acta, 50, 1379–1396.

———(1986b) Cathodoluminescence and minor elements in forsterite from extraterrestrial samples. American Mineralogist, 71, 966–970.

———(1988a) Enstatite cathodoluminescence: Assignment of emission peaks to Cr and Mn and application to quantitative analysis. Meteoritics, 23, 303.

———(1988b) Mineralogy of meteorites revealed by cathodoluminescence. In L.M. Coyne, S.W.S. McKeever, and D.F. Blake, Eds., Spectroscopic characterization of minerals and their surfaces, American Chemical Society Symposium Series 415, p. 150–164, American Chemical Society, Washington, D.C.

———(1989) Compositions of isolated forsterites in Ornans (C3O). Geochimica et Cosmochimica Acta, 53, 2069–2080.

———(1992) Olivine in Antarctic micrometeorites: comparison with other extraterrestrial olivine. Geochimica et Cosmochimica Acta, 56, 2923–2929.

———(1995) Oscillatory zoning in meteoritic forsterite. American Mineralogist, 80, 823–832.

Steele, I.M., Smith, J.V., and Skirius, C. (1985) Cathodoluminescence, minor elements and zoning in forsterites from Murchison (C2) and Allende (C3V) carbonaceous chondrites. Nature, 313, 294–297.

Steele, I.M., and Smith, J.V. (1986) Contrasting forsterite compositions for C2, C3, and UOC meteorites; evidence for divergence from common parent. Lunar and Planetary Science, X, 822–823.

Sutton, S.R., Jones, K.W., Gordon, B., Rivers, M.L., Bajt, S., and Smith, J.V. (1993) Reduced chromium in olivine grains from lunar basalt 15555: X-ray absorption near edge structure (XANES). Geochimica et Cosmochimica Acta, 57, 461–468.

Sutton, S.R., Bajt, S., and Jones, S. (1996) In situ determination of chromium oxidation state in olivine from chondrules. Lunar and Planetary Science, XXVII, 1291–1292.

Sviridov, D.T., Sevastyanov, B.K., Orekhova, V.P., and Sviridova, R.K. (1973) Optical absorption spectra of excited Cr^{3+} ions in magnesium spinel at room and liquid nitrogen temperatures. Optics and Spectroscopy, 35, 59–61.

Taftø, J., and Spence, J.C.H. (1982) Crystal site location of iron and trace elements in a magnesium-iron olivine by a new crystallographic technique. Science, 218, 49–51.

Vasconcellos, M.A.Z., and Steele I.M. (1996) Cathodoluminescence of Murchison forsterite: Temperature dependence and structural implications. Lunar and Planetary Science, XXVII, 1359–1360.

Wood, D.L., Imbusch, G.F., MacFarlane, R.M., Kisliuk, P., and Larkin, D.M. (1968) Optical spectrum of Cr^{3+} ions in spinels. Journal of Chemical Physics, 48, 5255–5263.

Yamamoto, N., Spence, J.H.C., Hazelton, D., Higgs, A., and Bergh, M. (1983) A cathodoluminescence detection system for TEM/STEM. In G.W. Bailey, Ed., Proceedings of the 41st Annual Meeting of the Electron Microscopy Society of America, p. 146–147. San Francisco Press, San Francisco.